JOURNAL OF QUATERNARY SCIENCE (2020) 1–10 ISSN 0267-8179. DOI: 10.1002/jqs.3212

JQS Journal of Quaternary Science QRA Quaternary Research Association

Indirect dating of an olive tree planting event using luminescence of the sediments lying beneath the roots of the tree: a pilot study in the south-western part of Anatolia, Turkey

EREN ŞAHINER,[1]* GEORGIOS S. POLYMERIS,[1] M. ALTAY ATLIHAN,[2] SELCUK AKTÜRK[3] and NIYAZI MERIÇ[1]
[1]Institute of Nuclear Sciences, Ankara University, Ankara, Turkey
[2]Faculty of Science and Letters, Department of Physics, Pamukkale University Kınıklı Campus, Denizli, Turkey
[3]Faculty of Science, Department of Physics, Muğla Sıktı Kocaman University, Muğla, Turkey

Received 10 January 2020; Revised 24 April 2020; Accepted 29 April 2020

ABSTRACT: The aim of the present study is to attempt assessing the age of a monumental olive tree located between the Antique Cities of Militus (Didim-Aydın region) and Iasos (Milas-Muğla region). Wood from the trunk of an olive tree is not appropriate for conventional dating approaches such as dendrochronology or ^{14}C. The sediments closely located surrounding and beneath the roots of the olive tree are considered indicative of the age of the planting event; therefore these sediments were dated using both quartz and feldspar luminescence signal protocols. Methodological aspects including the preheating plateaus, equivalent dose statistical approaches and dose rate using gamma spectrometry are also discussed, as dating of the associated palaeochannel sediments of the area are presented for the first time in the dating literature. The optically stimulated luminescence and/or infrared stimulated luminescence ages are extrapolated to date the event of the tree planting; it is the first time in the literature that an age is reported for an olive tree in the eastern Mediterranean region. The present study stands as the first experimental evidence that olive trees have been cultivated in the area since the Iron Age. Copyright © 2020 John Wiley & Sons, Ltd.

KEYWORDS: Aegean region; Anatolia; infrared stimulated luminescence; olive tree; optically stimulated luminescence.

Introduction

The olive tree is a long-lived species of fruit tree considered a reliable indicator of the Mediterranean environment (Moriondo *et al.*, 2013). The olive tree belongs to the species of small trees in the family Oleaceae, found mostly in the Mediterranean Basin from Portugal to the Levant, the Arabian Peninsula, southern Asia as far east as China, as well as the Canary Islands and Réunion. The word 'olive' derives from the Latin ŏlīva ('olive fruit', 'olive tree'), (Lewis *et al.*, 1969) possibly through the Etruscan 𐌄𐌋𐌄𐌉𐌅𐌀 (eleiva) from the archaic proto-Greek form. Olive is one of the most prevalent fruit, especially in ancient Israel and the Hebrew Bible, in the ancient Greek, Roman and Ottoman periods over the Mediterranean world and it is a vital component of both the Mediterranean culture and the Mediterranean diet. Although there is no tangible proof regarding its origin or the exact time when it became part of domestic agriculture in the Aegean region, Anatolia is accepted as an olive tree heartland. Cultivation of olive trees began around 6000 BC around Mesopotamia and Anatolia and it spread from there to the Mediterranean and Middle East territories. The olive tree has played a key role in human cultural and economic life and it can live up to several thousand years (Cline, 2010). The ancient Aegean people smeared olive oil all over their bodies and hair as a matter of grooming and good health. Olive oil was used to anoint kings and athletes in the ancient Hellenic period. It was burnt in the sacred lamps of temples and was the fuel of the 'eternal flame' of the original Olympic games. Victors in these games were crowned with its leaves. Moreover, olive is one of the holy plants across the Semitic religions, together with figs, persimmons, grapes and pomegranates.

Archaeological investigations that can provide detailed information about the history of olive cultivation as well as both the production and trade of olive oil in Anatolia are still open for study. It is understood from the Hittite texts that olive cultivation was very common on the Cilicia plain (Çukurova) (Vossen, 2007). During the excavations at Limantepe Höyük in Urla, İzmir, small hand mortars, grinding stones, soil containers for separating olive oil and later oil storage tanks were collected. Mortars and grinding stones were used for crushing olive pits. All these historical artefacts were dated between 3000 and 2000 BC. A sunken boat uncovered by marine archaeologists in Uluburun, off the coast of Kas in Antalya, was thought to belong to the Late Bronze Age (1200–2000 BC). It is estimated that this Late Bronze Age merchant ship, which sank in Uluburun about 3300 years ago, probably carried cargo from Ugarit to the Mycenaean Palace. This cargo included pomegranates, figs, grapes, almonds, pine nuts, wheat, barley and, last but not least, olives and olive oil. It is believed that some of these were transported for trade purposes and some of them were kept to meet the daily needs of the crew (Pulak, 1993). Archaeological documents provide further clues that there was a trading network including ships that were moving westward from the eastern Mediterranean (Levant region) to the Aegean (Vossen, 2007).

Although these earlier attempts provided some clues regarding the established know-how of olive cultivation and olive oil's production and trade, a critical aspect of the work, which is completely lacking, is the secure dating of olive cultivation. All the aforementioned studies provide indirect hints that olive cultivation and trade, along with olive oil production, was routine 5000 years before today in the Anatolian and ancient Greek regions. In this

*Correspondence: Eren Sahiner, as above.
E-mail: sahiner@ankara.edu.tr

context, age assessment of olive trees becomes extremely important for understanding Mediterranean civilisations. However, direct dating of olive trees from this specific region and period has not been reported so far in the literature. Although there is no clear consensus about the age and origin of the olive tree, according to most of the scientific literature, it originated in the area between Anatolia's Mardin, Kahramanmaraş and Hatay (Aktas, 2008). Note that Cherubini *et al.* (2013) emphasise that dendrochronological analyses of olive trees growing in the Aegean region are impractical due to various drawbacks such as intra-annual wood density fluctuations, cross-section and cambial activity problems. Additionally, Cherubini *et al.* (2014) have indicated that identification of olive-wood tree rings from Santorini by any means was found to be practically impossible. The core region of olive tree wood starts decomposing as it gets older (Ehrlich *et al.*, 2018). Therefore, wood from the core is not appropriate for analyses such as dendrochronology or ^{14}C dating (Cherubini *et al.*, 2013; Ehrlich *et al.*, 2018). Instead, taking a specimen from its roots and edge of the trunk is suggested for analysis purposes. Thus, age estimation based on either the stump rings, as is usually done with other trees, or with radiocarbon dating is not easy for the case of olive trees (Cherubini *et al.*, 2014). Generally, olive tree dating is performed using a gross estimation of the dimensions of the corresponding trunks; if the circumference of the olive tree trunk is larger than 10 m, then the tree is certainly very old. Therefore, regardless of whether the trees were accidentally or deliberately planted there by a human hand, finding the exact ages of these trees and their growing type are frequently debated. Whichever is the case, that olive seed sprouted and grew into a tree. Incidentally, dating of this type of tree by other methods could be problematic. Besides age estimation, the characterisation studies of olive trees are very scarce in the literature, including molecular investigation of monumental olive trees in the Apulia region (Salimonti *et al.*, 2013; Ninot *et al.*, 2018).

In the present study, an alternative, indirect way of assessing the age of an olive tree is attempted. It involves estimating the ages of sediments obtained from various points surrounding and beneath the roots of an ancient, monumental olive tree in the Aegean region of Turkey (Fig. 1a) and subsequently extrapolating these ages to the olive tree itself. To the best of the authors' knowledge, it is the first attempt to correlate the ages of sediments and planting of an olive tree in the related literature, despite the unconventional optically stimulated luminescence (OSL) dating applications reported so far, such as graves (Kemp *et al.*, 2014), sediment source (Wilkinson *et al.*, 2015) and rock art (Liritzis *et al.*, 2019). The ages of the sediments were evaluated using two different, albeit luminescent, techniques; namely, OSL of quartz and infrared stimulated luminescence (IRSL) signals of feldspar. Methodological aspects of the luminescent dating approaches, including preheating plateaux, equivalent dose statistical approaches and dose rate using gamma spectrometry are also discussed, as dating of the associated palaeochannel sediments of the area is presented for the first time in the dating literature. The implications of these ages for the social and economic life of the area in the past are discussed.

Materials and methods

Sampling site, archaeo-botanical and archaeo-sociological information

In the present study, a monumental olive tree (the locals call it '*Ata Ağaç*') was investigated in terms of age determination of the planting event using both OSL and IRSL dating techniques. This specific olive tree is located in the Aegean area of Turkey (Fig. 1a), about 60 km distance between the ancient Greek cities of Militus (Didim-Aydın region) and Iasos (Milas-Muğla region) on a mountain ridge formed along the Miletus (Milas) in the south-western part of Anatolia, Turkey (Fig. 1b). Both these antique cities have been recognised as UNESCO heritage monuments. They are important ancient Greek cities in the Carian Region (covering most of today's Aydın and Muğla provinces and the western end of Denizli). The tree is still active producing olives.

As a result of a preliminary evaluation performed by agricultural engineers from the relevant Turkish Ministry, the age of the tree is expected to be at least 1500 years old, based on the size of its trunk. As can be seen in Fig. 1b, the perimeter of the trunk at the ground level measures around 12.5 m. Moreover, its olive and leaf morphology, as well as the olive oil characteristics, are quite similar to those from olive trees from the eastern part of Crete (Lux, 2019). In Crete there are many ancient olive trees that are approximately several thousand years old that have been declared monumental by the Association of Cretan Olive Municipalities (Vossen, 2007). The distance of the sampling site from the sea is almost 150 km (Fig. 1a). Moreover, according to the information obtained from written sources and archaeological studies carried out in the Mediterranean region, the ancient people of the region were related to the Cretan culture, the trade of olives, olive oil and olive saplings from Crete (Cline, 2010). The presence of trading pathways between Crete and various Carian regions, including both Militus and Iasos, has been historically established to be earlier than the 4th century BC. Therefore, knowing the ages of this sort of tree is quite important to olive oil history research. Moreover, it is important to designate this territory as an archaeological site in order to protect it from misuses of agriculture. To find additional information on the geoarchaeological and historical context of the sampling area, the readers could refer to Cline (2010).

Sampling and chemical treatment

The aim of the present study is to extrapolate the sediments' ages to the age of the olive tree following planting. For this reason, two sediment samples were collected near the root of this olive tree, very close to the main trunk. The exact sampling stratigraphy related to the roots of the tree is shown in Fig. 1b. Moreover, four additional samples were collected, each one from cardinal points related to the trunk position (N, E, S and W). A total of six sedimentary samples were obtained with cylindrical metal opaque stainless-steel tubes (7.5 cm wide and 20 cm long), obeying conventional sampling protocols for OSL dating (Aitken, 1998; Şahiner, 2015). The codes of the samples are shown in Table 2, with these codes being characteristic of the sampling stratigraphy.

According to field observations, the climate of the region indicates gradual low energy deposition of slope deposits, providing adequate intervals for sun bleaching. However, a supplementary geological survey is required to get more detailed information from the region. Therefore, there are no obstacles in both terms of luminescence dating mechanism or bleaching ability anticipated from the studied territory.

The appropriate minerals for luminescence dating (feldspar and quartz) were meticulously isolated at subdued red-light filter conditions, employing proper chemicals and heavy-liquid separators (Mejdahl and Christiansen, 1994). The protocol includes the following steps: (1) handling of the bulk sediment using Hydrochloric acid (HCl) and Hydrogen peroxide (H_2O_2) (10%) in order to eliminate carbonates and organics until reactions finish; (2) magnetic separation utilising neodymium magnets; (3) wet-sieving for choosing the suitable grain-size fractions; grains with dimensions of between 90 and 140 μm were eventually selected; and (4) heavy-liquid separation using the sodium polytungstate suspension by

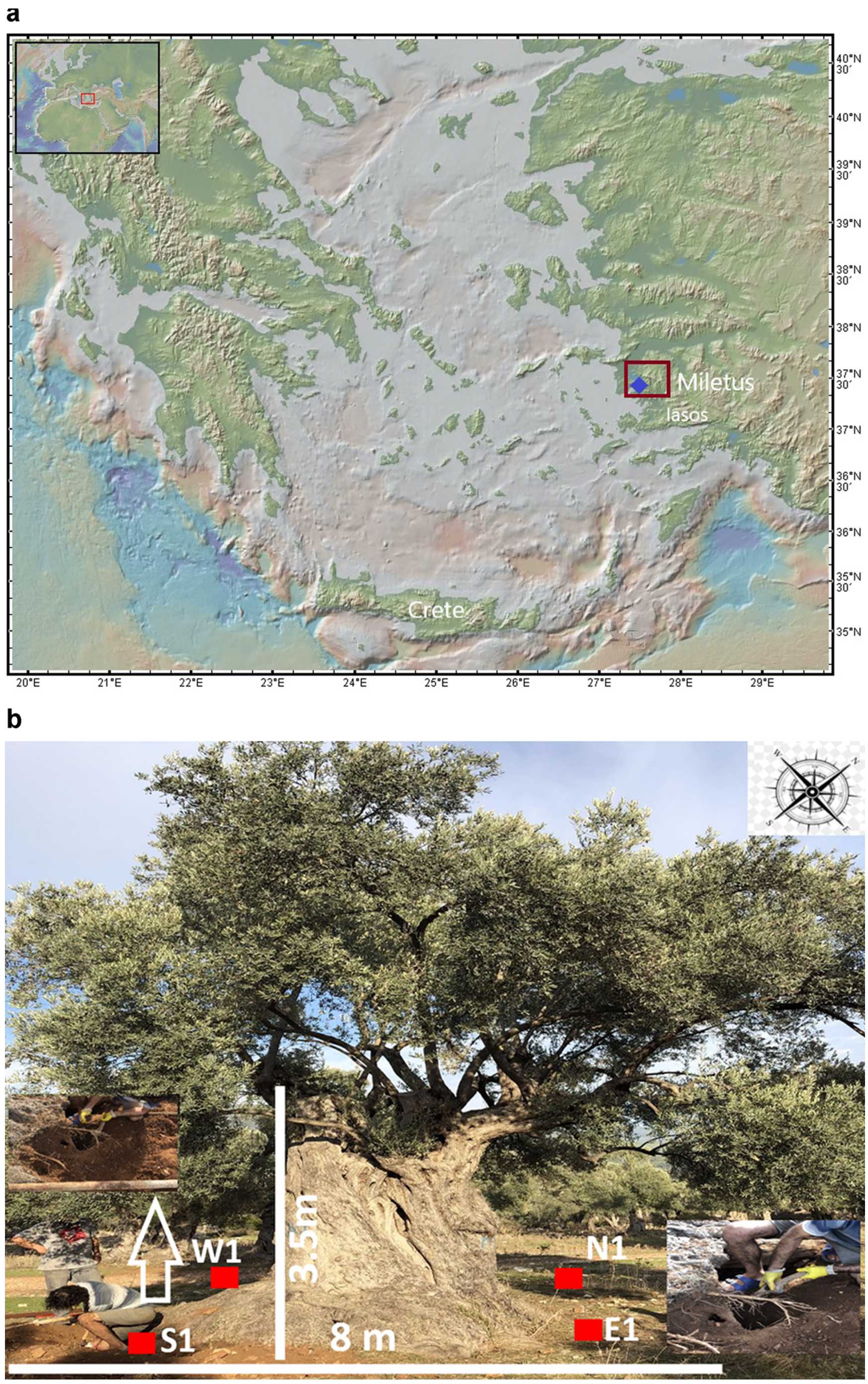

Figure 1. (a) Location map of the study area in Aegean Anatolia, (b) view of the prehistoric olive tree. Arrows indicate the sampling points (N1, S1, E1 and W1) and two more samples (R1 and R2) were collected beneath the roots using long metal opaque tubes. The tree still produces olives.

measured density (2.70; 2.62; 2.58 g cm^{-3}) to isolate heavy minerals such as quartz, apatite, zircon, etc. The quartz grains then underwent surface etching for 60 min in Hydrofluoric acid (40%, ~20 µm alpha dose affected parts) and were ultimately treated with HCl (10%) to remove any unsolvable fluorides after the malign effect of the fluoric acid. The prepared mineral grains were deposited on stainless-steel discs; around 1000 grains were deposited on each aliquot. Feldspathic contamination on separated quartz minerals was checked by IR stimulation at ambient temperature due to quartz traps not being sensitive to IR at room temperature.

Luminescence apparatus

All luminescence measurements were performed using a Risø thermoluminescence (TL)/OSL reader (model TL/OSL-DA-20), equipped with a ^{90}Sr/^{90}Y source delivering (0.114 ± 0.005 Gy/s: calibrated using reference quartz samples from the Risø National Laboratory) at the irradiation position together with a 9635QA PM Tube for light detection. The stimulation wavelength is 470 (±20) nm for the case of blue stimulation and 875 (±40) nm for the infrared stimulation. The filters for detection contained a 7.5 mm Hoya U-340 filter for the case of OSL from quartz minerals and a blue filter pack (combining a Schott BG-39 with Corning 7–59) for IRSL from feldspars. All heating was performed in a nitrogen atmosphere with a low constant heating rate of 2 °C/s, avoiding significant temperature lag (Kitis *et al.*, 2015). All blue/IR stimulation was carried out in a continuous wave configuration and the power level was software-controlled and set at 90% of the maximum stimulation intensity; 10 data points were received for each second of stimulation. The samples were mounted on stainless-steel cups, in a single-layer pattern; typical treatment and preparation were undertaken in subdued red-filtered light conditions. Background subtraction was applied following the suggestion of Şahiner *et al.* (2018).

Optically stimulated luminescence dating: rationale and experimental protocols

In general, luminescence dating and accidental retrospective dosimetry is based on the fact that naturally occurring minerals like quartz and feldspar act as natural dosimeters and preserve a record of irradiation dose received through time. This dose results mainly from the decay of natural radionuclides, i.e. ^{232}Th, ^{40}K, ^{87}Rb and natural U, along with cosmic rays (Aitken, 1985, 1998; Bøtter-Jensen *et al.*, 2003; Liritzis *et al.*, 2013). The brightness of the luminescence signal reflects the amount of trapped charge. Consequently, it is also proportional to the total irradiation dose accumulated in the sediment since its burial. Towards the direction of age determination, two different physical quantities are required; the total accumulated dose during the past, termed as the palaeodose or equivalent dose (ED), as well as the rate at which this energy dose is accumulated, termed the dose rate (Aitken, 1998; 1985). The age can be determined by dividing the ED over the dose rate:

$$Age(kyr) = \frac{ED(Gy)}{DR\left(\frac{mGy}{yr}\right)} \tag{1}$$

In the framework of the present study, the event to be dated is the planting of the tree. The sediments closely located both surrounding and beneath the roots of the olive tree are considered to indicate an age very similar to the age of the planting event. Therefore, the first aim is to date the palaeosediments close to the root of the tree; these ages will subsequently be extrapolated to the planting event. A similar OSL dating approach was recently adopted by Pietsch *et al.* (2019). In a multi-method approach to dating the burial event of Kiacatoo Man in New South Wales, Australia, these authors also calculated the OSL ages of the grave infill sediments, the underlying level and associated palaeochannel sediments. If the root of the olive tree in the present study was not of organic content but instead was a fossil root cast, the approach of rhizolith dating using TL could have been applied according to Polymeris *et al.* (2016).

The single-aliquot regeneration (SAR) protocol (e.g. Murray and Wintle, 2000) has permitted ED estimates to be obtained from subsample aliquots made up of a few hundred grains or a few dozen, and even from single grains (e.g. Galbraith *et al.*, 1999) The sequence of calculating ED using the SAR procedure is illustrated in Table 1 for both quartz (a) and feldspar (b) samples. It contains natural luminescence signal (L_N) measurements arising from natural irradiation, sensitivity assessment of the aliquot by luminescence signal (T_N) engendered by a test dose (Tx), an illumination step for erasing the residual signals and then repeating a number of cycles with increasing doses, each of which includes artificial irradiations (D_1, D_2, …,) to regenerate the luminescence signal (L_1, L_2, …,), followed by test doses (T_1, T_2, …,).

A minimum number of 24 aliquots and the central age model were used in order to estimate equivalent doses due to the central age scattering statistics. Six SAR cycles with increasing artificial doses were incorporated in order to construct the dose–response curve, along with a zero-dose cycle for the regeneration test and a repeat-dose for the recycling ratio test, each calibrated for sensitivity with a test dose as described in detail by Murray and Wintle (2000). The regeneration doses were 0, 0.6, 2, 7, 15, 30, 60 Gy, while the test dose was 5 Gy for both the OSL and IRSL signals.

For the IRSL, equivalent doses were corrected for athermal fading by incorporating the appropriate fading rate in percentage per decade, g value (Aitken, 1985) for each IRSL stimulation mode. The g values of each IRSL were determined according to the method by Huntley and Lamothe (2001), using the same time integration interval for both the ED and the g-value calculation. Besides the ED, the g value varies versus time-integration interval, implying that different g values were applied for correcting ages obtained for different time-integration intervals. Due to the relatively lower ages for IRSL, g values were calculated, indicating very low values with high associated errors (e.g. -0.1 ± 1.1, 0.13 ± 0.8 for N1 and R1 samples, respectively). Therefore related g values are neglected throughout the study. It is worth mentioning that two different IRSL signals were measured; namely, conventional IRSL measured at 50 °C as well as a postIR-IRSL signal measured at 290 °C. The original intention was to use the latter signal for the ED (and thus age) calculation. However, as seen in Fig. 2, the corresponding postIR-IRSL sensitivity was much fainter than the conventional IRSL signal. Such a feature is not so frequent in the luminescence dating literature using feldspathic minerals and could be attributed to the lack of K-feldspar and the possible presence of other types of feldspar; nevertheless, the lack of X-ray diffraction patterns excludes a strong experimental argument. Furthermore, this awkward result could be related to trapped-charge distribution throughout the relatively young aged feldspar crystal lattice, which needs further theoretical and experimental research. Therefore, the conventional IRSL signal, measured at 50 °C, was used for the age assessment.

Dose-rate assessment

The total dose rate was estimated from the natural radioactivity of the sediments, along with the cosmic ray contribution, using dose-rate components (Aitken, 1985, 1998). Regarding the radionuclide concentration, experiments were performed using a coaxial p-type high-purity Germanium (HpGe) detector (by ORTEC) which has 33% relative efficiency. Both calibration and activity calculation details of the detector have been described in a previous report by Şahiner and Meriç (2014). The content of natural U, ^{232}Th and ^{40}K along with the derived annual dose rates for both quartz and feldspar (the alpha, beta, gamma and cosmic ray dose rates) are presented in Table 2, which also includes water content (*W*), being an important factor in the dose absorption of sediments when calculating dose rates. Because water uptake during burial plays a significant role in the absorption of the radiation, saturation water content measurements were taken 0.6 ± 0.2, as in Aitken (1985).

The total annual dose rates together with internal dose rates and a luminescence age determination summary were comparatively calculated using an online calculator published by Durcan *et al.* (2015) and a user-friendly application published by Tsakalos *et al.* (2016) (as shown in Table 2).

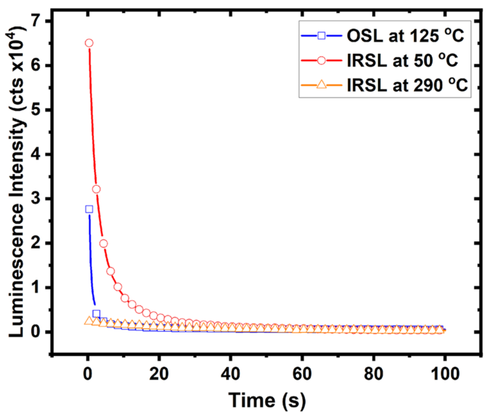

Figure 2. OSL and IRSL signals of quartz (squares) and feldspar (circles and triangle) minerals respectively, after isolation from sediments at related measurement temperatures after chemical procedures.

Moreover, Rb concentration has been estimated from K% concentration for each sample as stated by Huntley and Baril (1997). The internal dose rates for all feldspar samples are almost similar, varying from 0.22 ± 0.03 to 0.31 ± 0.04 mGy/a.

Luminescence methodological results

Figure 2 shows typical naturally occurring OSL and IRSL signals of the R1 sample as representatives for all other corrected samples. The signals may be considered bright enough, so it is straightforward to assume that the luminescence clock works. As anticipated, quartz mineral showed a very rapid discharge while feldspar mineral showed a slower, albeit still fast, discharge. Specific methodological issues regarding the application of the SAR protocol are presented in the following sections. These include preheating studies and the general methodological concerns of the ED calculation.

Preheating studies

A necessary initial step in both the OSL and IRSL methodologies is the elimination of the thermally unstable signal components using appropriate preheating procedures. Prior to each OSL/IRSL measurement, aliquots should be preheated to remove any unstable charge and to equalise the charge transfer between the natural and laboratory-irradiated charge populations. Even though there is no consensus in the related literature as to the beginning of the luminescence dating applications, it is agreed that preheating temperatures for common minerals such as quartz and feldspar are 200–260 °C and 250–320 °C for OSL and IRSL procedures, respectively, while the preheating duration is 1–10 s in both cases. Both parameters are sample-dependent for both minerals.

The so-called preheating plateau test stands as the most appropriate procedure for selecting the optimum preheating temperature. Despite the fact that the preheating plateau test is included in routine SAR OSL applications, the corresponding results are rarely presented in the literature. This latter test was applied for both quartz and feldspar minerals in the current study. The SAR protocol was applied to a number of aliquot groups; for each group a different preheating temperature was applied, ranging between 0 and 350 °C. Finally, the luminescence emission (normalised over mass) was measured and plotted against the preheating temperature (Fig. 3(a) and (c)). The optimum temperature was selected from the plateau regions of these plots. For the optimum preheating duration, a procedure similar to that explained above was followed, using the selected preheating temperature according to the previous experiment and changing the stimulation times (Fig. 3(b) and (d)). According to Fig. 3, the preheat values are calculated as 210 °C for 10 s for quartz mineral and 220 °C for 600 s for feldspar mineral.

ED calculation

The majority of the discs yielded luminescence signals with test results approved by all SAR criteria. EDs were calculated relying on individual dose–response curves, as illustrated in Fig. 4(a) and (b) for quartz and feldspar, respectively. Therefore, these aliquots were selected for ED calculation and the central age model (CAM) was applied, providing average ages for all samples. Some ED values were removed as outliers; these were less than the 10% of the total number of measured aliquots. The ages of the six samples are presented in Table 2. For well-bleached samples such as the case of the present study, the CAM is commonly used throughout the related literature (for examples the readers could refer to Fattahi *et al.*, 2016). Because there was no bleaching problem in the sediment nature of the study area and mineral used, the CAM model could be used to evaluate the upper side of the common luminescence age equation (Equation 1).

Furthermore, dose recovery tests (as applied in Murray and Wintle, 2000) were performed. Dose recovery results, lying within 8% of unity for all aliquots, indicate the suitability of the specified SAR procedure to successfully recover the given dose delivered to our samples. Moreover, the overall effects of sensitivity changes were properly corrected using pre-defined laboratory doses during the SAR protocols (Table 1(a) and b) and the mean ratios measured to given doses for either OSL or IRSL were statistically taken into account. This suitability is also strongly supported by the values of both the recycling ratios, which lie in the range 0.91–1.15, and the recuperation, which is less than $6.6 \pm 7.3\%$.

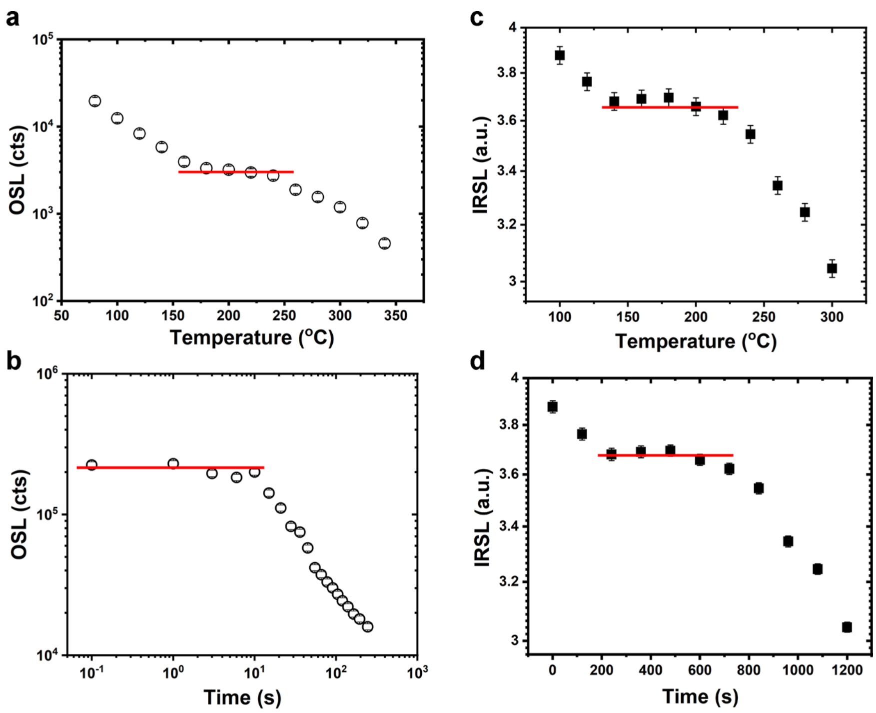

Figure 3. Preheat study for both quartz (a, b) and feldspar (c, d). Preheat parameters were selected from the plateau regions (red lines) at 210 °C, 10 s for quartz mineral and 220 °C, 600 s for feldspar mineral. It is applied for sample R1 in order to represent all samples.

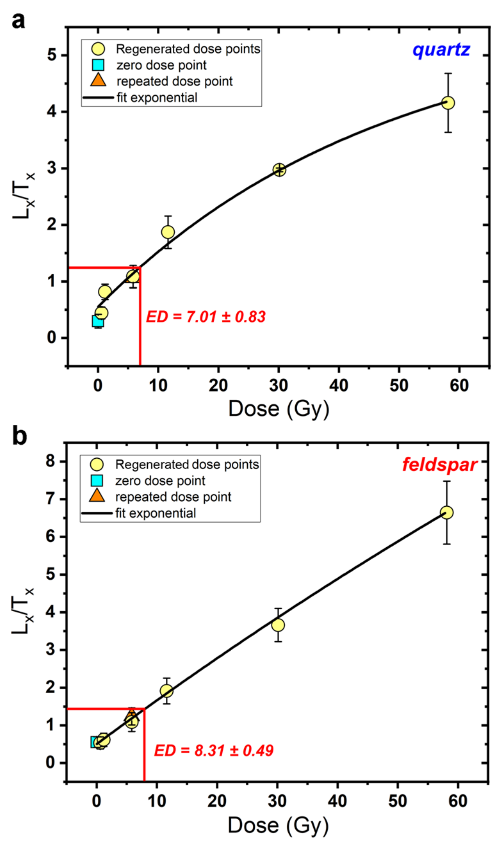

Figure 4. Representative SAR dose recovery graphs of selected aliquot of sample E1 for (a) quartz and (b) feldspar. All curves are fitted to an exponential function.

The single-aliquot ED distributions for each sample are displayed in Fig. 5 as abonico plots. The spread of the EDs could be related to 'experimental and natural' variations. Even though experimental errors are low, natural disparity is inherent in the nature of the material. Overdispersion values of up to ~20% among the considered ED values of the individual aliquots, indicate well-bleached sediments (Roberts *et al.*, 2000). The selected grain size of the minerals is a significant issue for calculating both annual dose rates and equivalent doses. As seen from the abonico plots in Fig. 5, heterogeneity in the dose values of some aliquots can be observed which might come from the used grain sizes (90–140 µm) over the study.

As Fig. 5 reveals, ED values, being directly proportional to OSL ages, are regularly scattered for both quartz and feldspar minerals over all samples, due to the geomorphology of the territory. Estimated ED values vary from 5 to 10 Gy for the majority of the aliquots. Other higher scattered ED values were not considered for the determination. According to Fig. 5, samples show more or less similar ages, excluding the second sample from the root (root2); the age of this sample is higher as the corresponding annual dose is relatively lower than the others.

Luminescence ages and implications

The age of all samples was calculated according to Equation 1 and the quoted errors denote 1σ uncertainties. The error calculation was performed according to Aitken (1985) and includes all quantifiable error sources. Luminescence dating results, including radioactive concentrations of sediments taken from the basin of the aged olive tree, are given in Table 2. It can be said that ages are subgrouped in terms of location; one group at the surface and one at the root. Root samples yield around 0.5 ka older ages from layer samples from different directions. While the ages of quartz are in the range of ~2–3 ka, the ages of feldspar are 2.1–3.2 ka BP. Age overestimation of feldspar mineral is in the range of ~0.2 ka. Based on the calculated ages, it is indicated that the last bleaching of the sediments, which in turn is related to the timeline of the olive tree implantation, whether artificial or natural, is chronologically located in the era of the Iron Age/ Ancient Greece, an era which led to developments in agricultural production. Even within error limits, the ages are compatible with the latter era. Moreover, the age that was revealed using luminescence stands in agreement with all independent, indirect evidence based on historical sources and relic objects related to olive cultivation, olive oil production, storage and trading. These ages testify to the antiquity of olive cultivation in the Mediterranean region, as well as the long lifespan and ability of these trees to survive under adverse conditions.

The results of the present study highlight the independent trajectories that were followed in the eastern Mediterranean region and as such stress the need for a more complete understanding including both socio-economic and technological parameters. This specific region has been one of the most important olive and olive oil producing regions in antiquity still in use today. It has been independently suggested that olive tree cultivation started on the island of Crete around 4000 BC. Texts in Linear B provide evidence for the production of olive oil in the Bronze Age (Vossen, 2007). Significant quantities of oil were stored in the palaces of Crete and its trade was the source of power and wealth of the kings of Crete among the Mediterranean countries (Diler, 1993). The ruins of a workshop dated to the Minoan Period (2800–1050 BC) showed that the printing press was produced in Crete during the Bronze Age (Cline, 2010). Even though the trading pathways of both olives and olive oil are known to have been extensive and far-reaching (Vossen, 2007), there is little archaeological evidence available to verify that olives were cultivated and olive oil was produced in the wider area. The present study provides such proof, as it is the first ever reported age of an olive tree. Of course, the olive tree in the present study is located in Anatolia, some hundred kilometres from both the sea and the eastern part of Crete. This close distance, in conjunction with olive and leaf morphologies as well as the olive oil characteristics, which are quite similar to the corresponding characteristics of olive trees from the eastern part of Crete, provide strong arguments for the fact that similar, if not the same, species of olive trees were cultivated in the specific wider area. This could have been achieved either deliberately, via the trading pathways between Crete and Militus, Iasos and other Carian Antique Cities, or alternatively via the wind-blown pathway.

There are many species of trees in the world that can reach ages of more than 1000 years, (Thomas, 2003, http://www.rmtrr.org) and the olive tree is one of the most important for mankind and civilisation. Olive tree cultivation dates back more than 6000 years, to the beginning of the farming era around Mesopotamia and it later spread westwards throughout the Mediterranean territory and along the Anatolian coasts (Terral *et al.*, 2004). Olive tree cultivation, along with the export of the corresponding products, was crucial for the people residing in the region. Thus, many technological developments have been made towards the more efficient use of olive products. In particular, the Miletus region was one of the leading places in this regard. Moreover, the oil of this region was famous from early times in Aristotle's works describing the story of Thales about making a large profit on a transaction of olive oil (Michell, 2014). Specifically, the trade

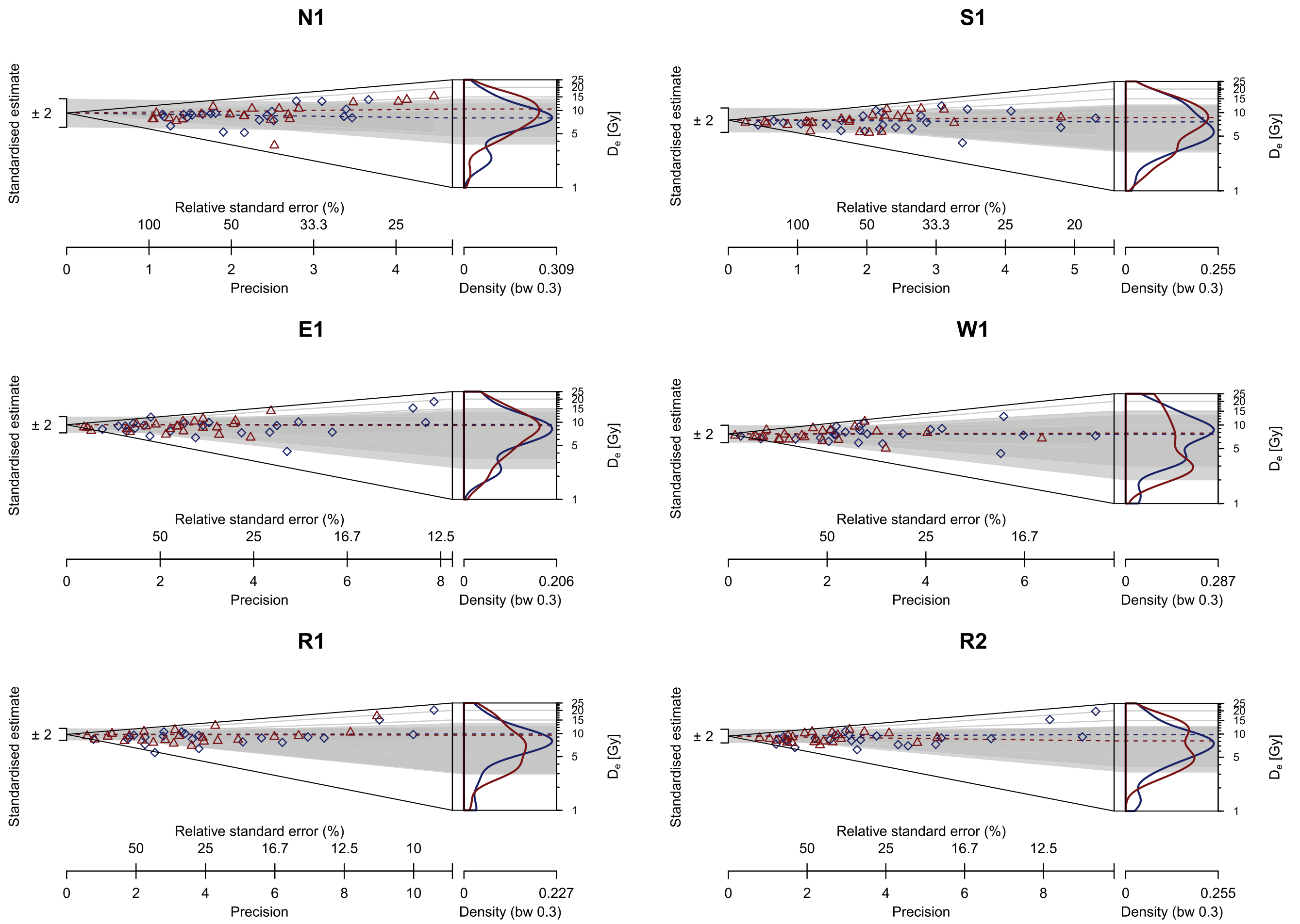

Figure 5. The ED values of all samples, in illustrative abonico plots (the combination of a radial plot and a kernel density estimation) of single-aliquot total absorbed dose distributions of both minerals as blue and red circles indicating quartz (diamond, ◊) and feldspar (triangle, Δ), respectively. The grey bands show values of scatter polygon from the CAM (central age model) estimation. Overdispersions for all samples vary between 17 and 26%, which are suitable for using CAM.

of olives and their products starts from 1000 BC becoming increasingly important to the economy of the region. Many written sources, including Holy books, talk about its mercantile benefits. Egyptian sources indicate that they were importing Milesian oil around the third century (Michell, 2014). The aforementioned studies show that the olive tree and all its products were essential for the economy of the Mediterranean territory 2–3 ka years ago. In fact, the situation did not dramatically change and olive products are still an important part of the economy throughout the Mediterranean.

The monumental olive tree that was the subject of the present study is believed to have been planted by hand in the context of a conscious agricultural procedure. Even though there is no reference suggesting this, there are various independent, indirect indications for it: (a) as Fig. 1(b) shows, the monumental tree is located in a field with other olive trees; moreover, the distance of this specific tree from the others is the same as the distance between any other neighbour olive trees in the same field, indicating a regular planting pattern; (b) in order to grow properly, the olive tree requires a hole of at

Table 1. Applied single-aliquot regenerated (SAR) sequences for both (a) OSL and (b) IRSL signals. Observed Lx and Tx are derived by integrating over the initial signal (5 s) minus a background estimated from the just after the signal (7–15 s) stimulation curve (Şahiner *et al.*, 2018). Corrected natural signal $N = L_0/T_0$; Corrected regenerated signal $Rx = Lx/Tx$ ($x = 1–6$). Note that in step 2, the sample has been heated to the preheat temperature using TL and held at that temperature for 10 s.

(a) SAR protocol for quartz			(b) SAR protocol for feldspar		
Step	Treatment	Observed	Step	Treatment	Observed
1	Give dose		1	Give dose	
2	Preheat 220 °C, 10 s		2	Preheat 220 °C, 600 s	
3	Stimulation with blue diods (125 °C, 40 s)	Lx	3	Stimulation with IR diodes (50 °C, 100 s)	Lx
4	Give test dose		4	Stimulation with IR light (290 °C, 100 s)	
5	Cut-heat TL (180 °C, 5 °C/s)		5	Give test dose	
6	Stimulation with blue light (125 °C, 40 s)	Tx	6	Cut-heat TL, 180 °C, 5 °C/s	
7	Illumination with blue light (280 °C, 100 s)		7	Stimulation with IR diodes (50 °C, 100 s)	Tx
8	Return to 1		8	Stimulation with IR light (290 °C, 100 s)	
			9	Illumination with IR light (325 °C, 100 s)	
			10	Return to 1	

Table 2. IRSL and OSL dating results for the monumental olive tree.

		Radionuclide concentrations							IRSL		OSL		ED (Gy) IRSL		ED (Gy) OSL		AD (mGy/a) IRSL		AD (mGy/a) OSL		IRSL Age (ka)		OSL Age (ka)	
		K		Th		U		burial depth (m)	OV (%)	Used aliquots	OV (%)	Used aliquots												
S. Code	S. Direction	%	error	ppm	error	ppm	error						value	error	value	error	value	error	value	error	value	error	value	error
N1	*north*	3.25	0.41	0.78	0.15	0.26	0.14	1.1	19	23/24	26	22/24	8.76	0.16	8.26	0.22	2.94	0.27	2.88	0.26	2.98	0.27	2.87	0.27
S1	*south*	2.5	0.19	0.46	0.11	0.14	0.09	0.8	21	24/24	23	23/24	6.36	0.12	5.76	0.18	2.27	0.14	2.24	0.14	2.80	0.19	2.67	0.17
E1	*east*	2.31	0.23	0.73	0.15	0.65	0.18	0.7	18	23/24	20	22/24	6.93	0.65	6.42	0.85	3.28	0.17	3.16	0.17	2.11	0.23	2.03	0.29
W1	*west*	2.6	0.25	0.67	0.16	0.36	0.14	1	17	23/24	22	23/24	5.90	0.18	5.60	0.28	2.46	0.18	2.39	0.19	2.40	0.18	2.34	0.20
R1	*root1*	3.54	0.21	1.21	0.18	0.53	0.12	1.2	20	23/24	21	22/24	9.93	0.23	8.26	0.35	3.31	0.17	3.21	0.16	3.00	0.18	2.58	0.25
R2	*root2*	2.45	0.22	0.49	0.11	0.47	0.12	1.5	17	23/24	18	23/24	7.52	0.28	6.78	0.56	2.37	0.16	2.29	0.15	3.17	0.28	2.96	0.35

least 75–100 cm in depth; these dimensions probably exclude accidental planting; and (c) cultivation of olive trees has been a routine conscious farming procedure in the area since 4000 BC. Based on this rationale, the age of the sediments closely surrounding and beneath the roots of the olive tree are considered indicative of the age of the planting event. This is why it is strongly believed that the event of the tree planting was dated. Nevertheless, even in the case that the olive tree was not consciously planted, the derived ages could be considered as a lower limit for the olive tree age, thus implying an even higher age for this specific monumental olive tree, closer to the Bronze Age.

Olive growing is one of the most important agricultural activities in the Mediterranean region. Ancient olive trees, including both cultivated and wild forms, are still found in several Mediterranean countries such as Italy (Erre *et al.*, 2010; Cicatelli *et al.*, 2013; Salimonti *et al.*, 2013), Greece (Cherubini *et al.*, 2013; Maravelakis *et al.*, 2013; Michelakis 2002), Montenegro (Lazović *et al.*, 2016), Spain (Ninot *et al.*, 2018), Israel and the Palestinian territories (Barazani *et al.*, 2014; Petruccelli *et al.*, 2014). The olive groves have played and still play a significant social and economic role and the ancient olive trees could be considered part of a living heritage. In this regard, inventorying, characterising and conserving ancient olive trees *in situ* should be considered a priority towards safeguarding their genetic, natural and agricultural value (Ninot *et al.*, 2018). Spain currently preserves a rich olive genetic heritage and a large local olive patrimony, conserving ancient olive trees *in situ* (Ninot *et al.*, 2018). In this recent study, more than 4500 productive, monumental olive trees from a highly important and well-preserved cultural landscape in north-eastern Spain were characterised at molecular and morphological levels, according to their genotype, trunk circumference, calculated age, biometrics, endocarp morphology, DNA markers and tree size in general. Similar ongoing projects are still pending in Italy (Salimonti *et al.*, 2013) and the western part of Greece, on the Ionian Islands. However, the area which includes the Greek islands (Crete, Rhodes, etc.) and the western coasts of Anatolia, Turkey, still lacks such a survey. As the current study reveals, this area includes a large number of monumental productive olive trees that are up to 3000 years old, comprising a unique living and exploitable part of botanical heritage. A study similar to that of Ninot *et al.* (2018) for the eastern Mediterranean region, dealing also with OSL ages and DNA markers, will possibly highlight the importance of these olive trees to the social and economic life of the area, especially in the past. Moreover, such a study will further establish the presence of historical trading pathways between Crete and various Carian regions. Nonetheless, such studies will possibly provide a first step for the conservation of these trees from spoliation, removal from their original locations and replanting in gardens for ornamental purposes, or even progressive transformation of traditional olive groves into modern ones.

Finally, as age assessment of olive trees using dendrochronology or ^{14}C techniques is difficult, the age of any olive tree could be estimated based on its trunk's circumference by means of the three most used algorithms: (1) radial growth rate 0.8–1.5 mm/year (Michelakis, 2002), using the highest growth rate considering the data on pollen dating and the main historical and climatic events, in order to avoid overestimations of the age; (2) age (y) = 5.3 × radius at a height of 1.0 m (cm) + 54.43 (Pannelli *et al.*, 2010); and (3) age (y) = 2.11 × diameter at a height of 1.3 m (cm) + 88.93 (Arnan *et al.*, 2012). While the upper limit of the calculation according to the algorithm of Michelakis (2002) stands in rough agreement with the calculated OSL age, the other two algorithms provide severe age underestimations, taking the OSL age of the present study as a reference. The effective application of OSL dating techniques to olive trees could possibly provide another, alternative algorithm which can relate the OSL age and the trunk's dimensions. Such a reference calibration curve could be constructed locally, for the olive tree cultural landscapes of each region/country; nevertheless, it could possibly expand universally. Of course, for such a calibration curve, either local or global, a large number of OSL ages would be required.

Conclusions

The importance of the olive in human history is included in all Holy books, in the Olympic Games traditions along with creation and foundation legends in Ancient Greek mythology. The archaeological and geological evidence also reveals that it has been used since 6000 BC. Nevertheless, the development and organisation of olive cultivation and olive oil production in the eastern Mediterranean region and its concomitant economic importance has rarely attracted scholarly attention. In the context of the present study, for the first time in the literature, the event to be dated is the planting of an olive tree in Turkey. The sediments both surrounding and beneath the roots of the olive tree are considered to be indicative of the age of the planting event. Therefore, the palaeosediments close to the root of the tree were initially dated using both OSL and IRSL; these ages were subsequently extrapolated to the planting event. The present study stands as the first experimental evidence that olive trees have been cultivated since the Iron Age in the eastern Mediterranean area. Our dating result stands in good agreement with the related literature about the presence of olive trees in the Iron Age and its spread across Aegean Anatolia and the Mediterranean. This is another example regarding the successful application of luminescence dating to another question of multidisciplinary interest. Further geological and archaeological studies are required in order to establish human trade and agricultural activity in the territory.

Acknowledgements. The authors want to acknowledge the valuable comments of anonymous reviewers for improving the quality of the manuscript. Moreover, the first author (ES) wants to dedicate this paper to all ancient civilisations that spent some time in the region.

Data availability statement

Data openly available in a public repository that issues data sets with DOIs.

References

Aitken MJ. 1985. *Thermoluminescence dating.* Academic Press: Orlando, London.

Aitken MJ. 1998. *Introduction to optical dating: the dating of Quaternary sediments by the use of photon-stimulated luminescence*. Clarendon Press: New York.

Aktas E. 2008. Zeytin Üretimindeki Gelişmeler ve Çanakkale. (in Turkish). Published in: Canakkale-Küçükkuyu Değerleri Sempozyumu (20 August 2008).

Arnan X, López BC, Martínez-Vilalta J, *et al.* 2012. The age of monumental olive trees (Olea europaea) in northeastern Spain. *Dendrochronologia* **30**: 11–14.

Barazani O, Westberg E, Hanin N, *et al.* 2014. A comparative analysis of genetic variation in rootstocks and scions of old olive Trees – a window into the history of olive cultivation practices and past genetic variation. *BMC Plant Biology* **14**: 146.

Botter-Jensen L, McKeever SWS, Wintle AG. 2003. *Optically Stimulated Luminescence Dosimetry*. Amsterdam, The Netherlands.

Cherubini P, Humbel T, Beeckman H, *et al.* 2013. Olive Tree-Ring Problematic Dating: A Comparative Analysis on Santorini (Greece). *PLoS One* **8**(1): e54730.

Cherubini P, Humbel T, Beeckman H, *et al.* 2014. The olive-branch dating of the Santorini eruption. *Antiquity* **88**: 267–273.

Cicatelli A, Fortunati T, De Feis I, *et al.* 2013. Oil composition and genetic biodiversity of ancient and new olive (Olea europea L.) varieties and accessions of southern Italy. *Plant Science* **210**: 82–92.

Cline EH. 2010. *The Oxford Handbook of the Bronze Age Aegean*. Oxford University Press.

Diler A. 1993. Akdeniz Bölgesi Antik Çağ Zeytinyağı ve Şarap İşlikleri. XI. Araştırma Sonuçları Toplantısı 1–20 (in Turkish).

Durcan JA, King GE, Duller GAT. 2015. DRAC: Dose Rate and Age Calculator for trapped charge dating. *Quaternary Geochronology* **28**: 54–61.

Ehrlich Y, Regev L, Boaretto E. 2018. Radiocarbon analysis of modern olive wood raises doubts concerning a crucial piece of evidence in dating the Santorini eruption. *Nature: Scientific Reports* **8** (2018): 11841.

Erre P, Chessa I, Muñoz-Diez C, *et al.* 2010. Genetic diversity and relationships between wild and cultivated olives (Olea europaea L.) in Sardinia as assessed by SSR markers. *Genetic Resources and Crop Evolution* **57**: 41–54.

Fattahi M, Heidary M, Ghasemi M. 2016. Employing Minimum age model (MAM) and Finite mixture modeling (FMM) for OSL age determination of two important samples from Ira Trench of North Tehran Fault. *Geochronometria* **43**: 38–47.

Galbraith RF, Roberts RG, Laslett GM, *et al.* 1999. Optical dating of single and multiple grains of quartz from Jinmium rock shelter, northern Australia: Part I, experimental design and statistical models. *Archaeometry* **41**: 339–364.

Huntley DJ, Baril MR. 1997. The K content of the K-feldspars being measured in optical dating or in thermoluminescence dating. Ancient TL, 15: 11–13. http://ancienttl.org/ATL_15-1_1997/ATL_15-1_Huntley_p11-13.pdf

Huntley D J, Lamothe M. 2001. Ubiquity of anomalous fading in K-feldspars and the measurement and correction for it in optical dating. *Canadian Journal of Earth Sciences* **38**(7): 1093–1106.

Kemp J, Pietsch TJ, Olley J. 2014. Digging your own grave: OSL signatures in experimental graves. *Journal of Human Evolution* **76**: 77–82.

Kitis G, Kiyak NG, Polymeris GS. 2015. Temperature lags of luminescence measurements in a commercial luminescence reader. *Nuclear Instruments and Methods in Physics Research Section B: Beam Interactions with Materials and Atoms* **359**: 60–63.

Lazović B, Adakalić M, Pucci C, *et al.* 2016. Characterizing ancient and local olive germplasm from Montenegro. *Scientia Horticulturae* **209**: 117–123.

Lewis CT, Freund W, Short C. 1969. *A Latin dictionary: founded on Andrews' edition of Freund's Latin dictionary*. Clarendon Press: Oxford.

Liritzis I, Bednarik RG, Kumar G, *et al.* 2019. Daraki-Chattan Rock Art Constrained Osl Chronology And Multianalytical Techniques: A First Pilot Investigation. *Journal of Cultural Heritage* **37**: 29–43.

Liritzis I., Singhvi AK., Feathers JK., Wagner AG., Kadereit A., Nikolaos Z., Li SH. 2013. *Luminescence Dating in Archaeology, Anthropology, and Geoarchaeology: An Overview*. Springer, Heidelberg: New York.

Lux H. 2019. Historic 3,000-year-old olive tree still producing olives to this day. Online article available at: https://www.good.is/articles/olive-tree-vouves-greece-crete. Accessed 10 January 2020.

Ninot A, Howad W, Aranzana MJ, *et al.* 2018. Survey of over 4,500 monumental olive trees preserved on-farm in the northeast Iberian Peninsula, their genotyping and characterization. *Scientia Horticulturae* **231**: 253–264.

Maravelakis E, Konstantaras A, Kritsotaki A, *et al.* 2013. Analysing user needs for a unified 3D metadata recording and exploitation of cultural heritage monuments system. In *Advances in Visual Computing, Pt Ii, Vol 8034. Lecture Notes in Computer Science*, Bebis G, Boyle R, Parvin B (eds). Springer-Verlag: Berlin; 138–147.

Mejdahl V, Christiansen HH. 1994. Procedures used for luminescence dating of sediments. *Quaternary Science Reviews* **13**: 403–406.

Michelakis N. 2002. Monumental Olive Trees in the World, Greece and Crete. *Olive and Oil in Crete, Proceedings of the International Symposium Sitia 23-25 May 2002*. pp. 32-43. Crete: Association of Olive Municialities of Crete.

Michell H. 2014. *The economics of ancient Greece*. Cambridge University Press.

Moriondo M, Trombi G, Ferrise R, *et al.* 2013. Olive trees as bio-indicators of climate evolution in the Mediterranean Basin. *Global Ecology and Biogeography* **22**: 818–833.

Murray AS, Wintle AG. 2000. Luminescence dating of quartz using an improved single-aliquot regenerative-dose protocol. *Radiation Measurements* **32**: 57–73.

Pannelli G, Pandolfi S, Baldoni L. 2010. Selezione e valorizzazione di olivi antichi in Umbria. IV Convegno Nazionale Piante Mediterranee. Le potenzialità del territorio e dell'ambiente. Raccolta degli Atti Sarli G, Alvino A, Cervelli C, Nova Siri Marina (Matera). pp. 93–104.

Petruccelli R, Giordano C, Salvatici MC, *et al.* 2014. Observation of eight ancient olive trees (Olea europaea L.) growing in the Garden of Gethsemane. *Comptes Rendus Biologies* **337**: 311–317.

Pietsch T, Kemp J, Pardoe C et al. 2019. A multi-method approach to dating the burial and skeleton of Kiacatoo Man, New South Wales, Australia. *Journal of Quaternary Science* **34**(8): 662–673.

Polymeris GS, Kitis G, Kiyak NG, *et al.* 2016. Dating fossil root cast (Black Sea coast, Turkey) using thermoluminescence: Implications for windblown drift of shelf carbonates during MIS 2. *Quaternary International* **401**: 184–193.

Pulak C. 1993. Ulu Burun (Kaş) Batığı Kazısı: 1991 Kampanyası. XIV. Kazı Sonuçları Toplantısı, CI, Ankara-25-29 Mayıs 1992 347–364. (in Turkish).

Roberts RG, Galbraith RF, Yoshida H, *et al.* 2000. Distinguishing dose populations in sediment mixtures: A test of single-grain optical dating procedures using mixtures of laboratory-dosed quartz. *Radiation Measurements* **32**: 459–465.

Şahiner E. 2015. TL/OSL and ESR Methods Used in Paleoseismology Studies: Kütahya-Simav and North Anatolian Fault Zone (Doctoral dissertation, PhD Thesis, Ankara University, (in Turkish).

Şahiner E, Meriç N. 2014. A trapezoid approach for the experimental total-to-peak efficiency curve used in the determination of true coincidence summing correction factors in a HPGe detector. *Radiation Physics and Chemistry* **96**: 50–55.

Şahiner E, Erturaç MK, Polymeris GS, *et al.* 2018. Methodological studies on integration time interval's selection for the luminescence ages using quartz and feldspar minerals; sediments collected from Sakarya, Turkey. *Radiation Measurements* **120**: 163–169.

Salimonti A, Simeone V, Cesari G, *et al.* 2013. A first molecular investigation of monumental olive trees in Apulia region. *Scientia Horticulturae* **162**: 204–212.

Terral JF, Alonso N, Buxó I, Capdevila R, *et al.* 2004. Historical biogeography of olive domestication (Olea europaea L.) as revealed by geometrical morphometry applied to biological and archaeological material. *Journal of Biogeography* **31**: 63–77.

Thomas H. 2003. Do green plants age, and if so, how? – In: Nyström, T. & Osiewacz, H. D. (Eds.): *Model Systems in Aging*. Springer: Berlin; 145–171.

Tsakalos E, Christodoulakis J, Charalambous L. 2016. The Dose Rate Calculator (DRc) for Luminescence and ESR Dating-a Java Application for Dose Rate and Age Determination. *Archaeometry* **58**: 347–352.

Vossen P. 2007. Olive oil: history, production, and characteristics of the world's classic oils. *HortScience* **42**: 1093–1100.

Wilkinson SN, Olley JM, Furuichi T, *et al.* 2015. Sediment source tracing with stratified sampling and weightings based on spatial gradients in soil erosion. *Journal of Soils and Sediments* **15**: 2038–2051.

